

Quantum Chemistry Studies of Glycine–H₂O₂ Complexes

Shan Xi Tian*

Hefei National Laboratory of Physical Sciences at Microscale, Laboratory of Bond Selective Chemistry,
Department of Chemical Physics, University of Science and Technology of China,
Hefei, Anhui 230026, People's Republic of China

Received: June 17, 2004; In Final Form: October 14, 2004

Twelve glycine–H₂O₂ complexes are studied at the density three-parameter hybrid functional DFT-B3LYP/6-31++G(d,p) level regarding their geometries, energies, vibrational frequencies, and topological features of the electron density. Natural bond orbital (NBO) analysis and the Bader's theory of atoms in molecules (AIM) are employed to elucidate the interaction characteristics in the complexes. These complexes except for **III-1** are doubly hydrogen bonding. The distinct cooperative effect and the typical resonance-assisted hydrogen-bonding mechanism are exhibited in the six-membered rings of complexes **I-1** and **II-1**. The binding energies play a central role in the relative stabilities of the complexes, among which **I-1** is the most stable conformer. A strength sequence of the hydrogen bonds from the strongest to the weakest is found: O–H···N, O–H···O, N–H···O, and C–H···O. The blue- and red-shifts in the local X–H (X = O, C, N) stretching frequencies are proportional to the bond elongations or shortening lengths. The NBO analyses show that the electronic charge is transferred from glycine to H₂O₂ in these complexes except for **I-1** and **II-1**. The electron density ρ at the hydrogen bond critical point predicted by AIM is strongly correlated with the hydrogen bond parameter $\delta R_{H\cdots Y}$ (the difference between the sum of the van der Waals radii of H and Y atoms and the length of hydrogen bond H···Y), the Fock matrix element F_{ij} in the NBO scheme, and the interaction energy of the complex.

1. Introduction

Oxidation in biological systems can damage biomolecules including nucleic acid and protein. Hydrogen peroxide (H₂O₂) generating highly reactive radicals has been proven to play a role in the oxidation reactions.¹ Significant quantities of H₂O₂ can be detected as a byproduct of several metabolic pathways in human blood.² The neutral H₂O₂ adducts can cross the cell membrane to interact with intracellular targets; for example, DNA bases in the mammalian cells can be modified by treating with H₂O₂.³ The interactions between DNA base adducts and H₂O₂ have been investigated theoretically at the ab initio level^{4–7} and by X-ray experiments.⁸ Moreover, theoretical studies have been carried out on a few systems of H₂O₂ dimer,^{9a,b} H₂O₂ interacting with water,^{9c} hydrogen halides,^{9d} and urea.^{9e} However, there are no theoretical reports on the interactions between protein and H₂O₂. Most researchers focus on the reactivity between protein and hydroxyl radical produced by UV radiation,¹⁰ and various products such as nitrate, ammonia, formic acid, and carbon dioxide have been detected.^{10,11} In fact, the formation of the intermediate or prereactive hydrogen-bonding complexes may influence considerably the kinetics of the reaction, and the hydrogen-bonding forces are sufficient to influence the collision dynamics as the reagents approach each other.¹²

On the other hand, there has been a rapid development of theoretical and experimental research on hydrogen bonds (HBs) in the last century. According to geometrical, energetic, thermodynamic, and functional properties, HB strength is usually classified into three or four levels.¹³ Recently, HBs were reviewed from a phenomenological point of view. X–H···Y

interaction can be a HB if (a) it constitutes a local bond and (b) X–H acts as a proton donor to Y.¹⁴ There is a formal or real electron transfer whose direction is reverse to the direction of proton donation. In particular, this charge transfer (CT) is provided by the interaction of the lone pair of the acceptor atom with the unoccupied σ^* orbital of the X–H donor.¹⁵ Glycine (NH₂CH₂COOH), as the prototype of protein, has been investigated extensively.¹⁶ In this work, the interactions in the glycine–H₂O₂ complexes in the gas phase will be investigated theoretically. Glycine can be both proton acceptor (O and N atoms) and donor (OH, CH, and NH groups). It is notable here that the weak HBs (e.g., C–H···O) play key roles in protein folding and molecular recognition.¹⁷ The three most stable conformers of glycine¹⁶ are considered in this work; see Figure 1. There are four directions for the hydrogen-bonding attack at the glycine molecular plane. Their HB strength and the contributions to stabilize the complexes are of interest in this work.

To analyze binding energy (ΔE) between two monomers in a pair complex, two methods based on the Morokuma model¹⁸ and natural bond orbital (NBO) theory¹⁹ are frequently applied for decomposing ab initio ΔE . The ΔE value can be decomposed as

$$\Delta E = \Delta E_{\text{prep}} + \Delta E_{\text{int}} \quad (1)$$

where the preparation energy ΔE_{prep} is the amount of energy required to deform the separate bases from their free monomer structure to the geometry that they acquire in the pair complex; the interaction energy ΔE_{int} represents the actual energy change when the prepared bases are combined to form the pair complex. In the Morokuma scheme, ΔE_{int} consists of the following

* E-mail: sxtian@ustc.edu.cn.

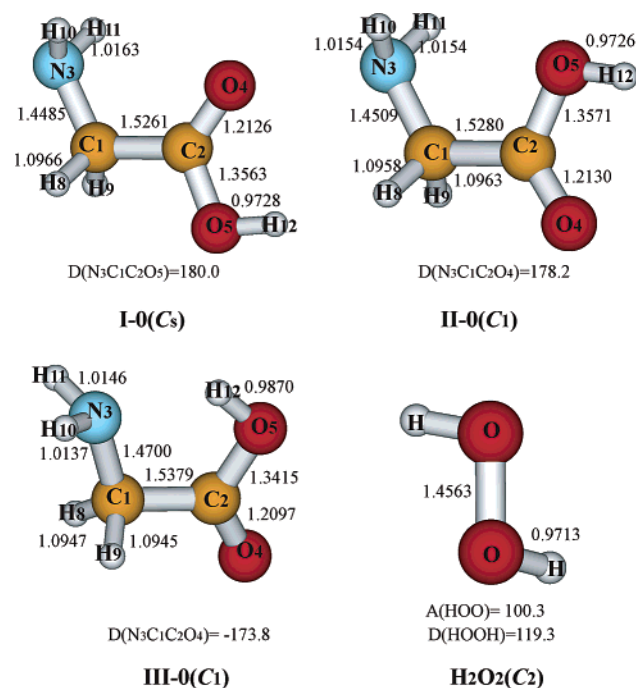


Figure 1. Geometrical parameters of free monomers (bond lengths in Å, angles in deg).

components: the term $\Delta V_{\text{e-stat}}$ representing the classical electrostatic interaction between the unperturbed charge distributions of the prepared bases, usually attractive, the Pauli term ΔE_{Pauli} responsible for the steric repulsion, and the orbital interaction ΔE_{oi} in any molecular orbital (MO) model accounting for the CT (ΔE_{CT}) and polarization (ΔE_{pol}) interactions.¹⁸ This situation becomes simple in the NBO scheme, and ΔE_{int} is decomposed into the CT and non-charge-transfer (NCT) parts,¹⁹

$$\Delta E_{\text{int}} = \Delta E_{\text{NCT}} + \Delta E_{\text{CT}} \quad (2)$$

Since the nonorthogonal MOs are used in the Morokuma model while those in NBO are orthogonal, the ΔE_{CT} in the Morokuma model is always smaller than that in eq 2.¹⁹ In fact, the electrostatic energy term plays a central role in the HBs according to the Morokuma analysis, which differs distinctly from the central role of the CT mechanism assigned by the NBO analysis. In this work, the NBO analysis will be made, and the ΔE_{CT} in the NBO scheme is used throughout this work.

2. Theoretical Methods

All structures were fully optimized at the three-parameter hybrid density functional DFT-B3LYP²⁰/6-31++G(d,p) level using the GAUSSIAN 98 package.²¹ The stability of each complex was examined by the analytic frequency calculations. It has been demonstrated that DFT-B3LYP and MP2 levels of theory give similar results;²² in particular, the B3LYP/6-31++G(d,p) method is very reliable for predicting the acidities of biological molecules.²³ The interaction energy, ΔE_{int} , was corrected for basis set superposition error (BSSE) by using the Boys–Bernardi counterpoise (CP) scheme.²⁴ The nucleic relaxation energy for each monomer, corresponding to ΔE_{prep} , was calculated by the difference of the total energy between free monomer and the corresponding moiety in the complex.

The electron density was calculated at the B3LYP/6-31++G(d,p) level and further analyzed by the NBO program.²⁵ The NBO analysis transfers the delocalized molecular orbitals into the localized ones that are closely tied to chemical bond

concepts. Filled NBOs describe the hypothetical, strictly localized Lewis structure. The interaction between filled as well as lone pair electrons and antibonding orbitals represents the deviation of the molecule from the Lewis structure and can be used as a measure of delocalizations due to hydrogen bonding in this work. Since the occupancies of filled NBOs are highly condensed, the delocalizing interactions can be further treated by the second-perturbation energies $E(2)$,

$$E(2) = -n_{\sigma} \frac{\langle \sigma | F | \sigma^* \rangle^2}{\epsilon_{\sigma^*} - \epsilon_{\sigma}} = -n_{\sigma} \frac{F_{ij}^2}{\Delta \epsilon} \quad (3)$$

where F_{ij} is the Fock matrix element between the NBO i (σ) and j (σ^*), ϵ_{σ} and ϵ_{σ^*} are the energies of σ and σ^* NBOs, and n_{σ} is the population (a lone pair in the HB).¹⁹ The topological features as far as the electron density ρ and its Laplace transform $\nabla^2 \rho$ at the HB critical points were calculated with the Bader's theory of atoms in molecules (AIM).²⁶

3. Results and Discussion

A. Geometrical Parameters and Energies. The geometrical parameters of free monomers for the most stable glycine isomers **I-0** (C_s), **II-0** (C_1), **III-0** (C_1), and H_2O_2 (C_2) are shown in Figure 1. Although the intramolecular HBs are known in these glycine isomers,¹⁶ we will focus only on the intermolecular interactions. Their energetic stabilities and molecular properties are presented for comparison with the glycine– H_2O_2 complexes shown in Figures 2, 3, and 4. We also tentatively searched the other stable conformers, but they were found to correspond to the unstable high-order points on the potential energy surfaces or to relax to the present ones. We could not locate the hypothesized conformer similar to **I-3** or **II-3** for **III-0**– H_2O_2 . The stable conformers except for **III-1** are doubly hydrogen bonding. Six-membered and seven-membered bonding rings are found in a set of complexes **I-1**, **I-3**, **II-1**, **II-3**, and the other set of **I-4**, **II-4**, **III-4**, respectively, exhibiting the existence of multiple interactions.

To give prominence to the characteristics of the complexes, we summarized the geometrical discrepancies of the complexes with respect to the free monomers in Table 1. The specific hydrogen bonding not only influences the lengths of the local bonds (to elongate or shorten) but also changes the other geometrical parameters. The glycine molecular plane is deformed markedly in **III-2**, while it is almost kept in **I-1**, **I-4**, and **II-2**.

As far as elongating or shortening the bond length due to hydrogen bonding, the different magnitudes for a certain bond are presented in Table 1, revealing the various strengths of the HBs. In particular, the six-membered ring of complex **I-1** exhibits the remarkable resonance-assisted hydrogen bonding (RAHB) mechanism.²⁷ Namely, the bond $\text{C}_2=\text{O}_4$ is elongated by 0.0131 Å, while the bond C_2-O_5 is shortened by 0.0185 Å, because of the two HBs $\text{O}_5-\text{H}_{12} \cdots \text{O}_6$ and $\text{O}_6-\text{H}_{13} \cdots \text{O}_4$, in which the bonds O_5-H_{12} and O_6-H_{13} are shortened by 0.0150 and 0.0156 Å, respectively. This mechanism is also found in complex **II-1**, where it seems a little more distinguished than the former. It is well known that the RAHB mechanism enhances the HB strength.²⁷ Moreover, the $\text{C}_1-\text{H}_8 \cdots \text{O}_7$ length in **I-3** is longer by 0.1678 Å than that in **I-4**, and that in **II-3** is longer by 0.2864 Å with respect to that in **II-4** (see Table 2). The differences can be explained by the following facts. There should be no or much weaker RAHB in complexes **I-4** and **II-4**, due to the more diffuse seven-membered rings. Somehow, the RAHB mechanism happens to weaken the $\text{C}_1-\text{H}_8 \cdots \text{O}_7$

TABLE 1: Geometrical Parameter Differences (elongate or widen: positive value; shorten or narrow: negative value) with Respect to Free Monomers (bond length in 10^{-3} Å, angle in deg)

	I-1	I-2	I-3	I-4	II-1	II-2	II-3	II-4	III-1	III-2	III-3	III-4
$R(C_1-C_2)$	-1.8	0.0	-5.3	-2.7	-1.5	1.1	-4.9	-3.1	-3.6	-1.1	-5.6	-4.1
$R(C_1-N_3)$	0.0	-6.7	11.0	-0.8	-0.6	-7.2	11.7	-1.6	-1.0	12.7	-3.7	0.6
$R(C_2=O_4)$	13.1	6.7	0.4	-3.7	13.5	-3.2	-1.8	8.7	6.1	2.0	-2.4	9.6
$R(C_2-O_5)$	-18.5	-7.8	-3.7	16.0	-19.8	14.5	0.8	-10.2	-9.4	-0.8	13.3	-11.3
$R(C_1-H_8)^a$	-0.1	-0.1	-1.1	-0.6	0.3	0.3	0.0	-1.2	-0.2	1.7	0.8	-0.6
$R(C_1-H_9)$	0.0	1.2	-1.4	0.7	0.0	0.7	-2.3	1.6	-0.3	-1.1	0.6	0.0
$R(N_3-H_{10})$	-0.1	-1.3	1.5	-0.3	0.2	-1.4	1.5	-0.4	0.1	4.3	0.1	-0.3
$R(N_3-H_{11})^b$	-0.1	0.5	1.2	-0.5	0.2	0.1	1.6	-0.3	-0.5	4.1	2.5	-0.4
$R(O_5-H_{12})$	15.0	0.3	-0.2	0.3	16.1	1.1	0.1	0.6	3.4	-0.2	5.6	4.8
$R(O_6-O_7)$	-2.1	0.2	4.8	1.1	-1.8	0.0	5.0	1.7	0.1	3.5	-1.8	0.8
$R(O_6-H_{13})$	15.6	11.7	25.4	5.9	16.8	6.7	24.7	12.0	11.0	38.2	8.2	16.6
$R(O_7-H_{14})$	-0.2	-1.1	-1.7	-0.9	-0.2	-0.7	-1.7	-1.2	-0.9	-1.1	-0.4	-1.1
$D(N_3C_1C_2O_{4,5})^c$	0.0	-5.8	-2.2	0.6	0.9	1.7	-7.4	-6.1	4.5	-44.0	-7.7	4.5
$D(H_{13}O_6O_7H_{14})$	-2.6	-6.5	2.4	-0.5	-3.2	-2.9	3.5	-5.0	-11.0	6.5	-10.9	-10.6

^a Involved in hydrogen bonding for **I-3**, **I-4**, **II-3**, **II-4**, and **III-4**. ^b Involved in hydrogen bonding for **I-2**, **II-2**, and **III-3**. ^c $D(N_3C_1C_2O_5)$ for **I-1,2,3,4**; $D(N_3C_1C_2O_4)$ for **II-(III)-1,2,3,4**.

TABLE 2: Geometrical Parameters of Intermolecular Hydrogen Bonds (bond lengths in Å, angles in deg)

I-1	$R(O_4\cdots H_{13}-O_6) = 1.8892$; $A(O_4\cdots H_{13}-O_6) = 140.9$; $R(O_5-H_{12}\cdots O_6) = 1.8709$; $A(O_5-H_{12}\cdots O_6) = 152.5$; $D(O_4O_6O_5C_2) = 0.1357$
I-2	$R(O_4\cdots H_{13}-O_6) = 1.8382$; $A(O_4\cdots H_{13}-O_6) = 176.0$; $R(N_3-H_{11}\cdots O_7) = 2.2037$; $A(N_3-H_{11}\cdots O_7) = 155.4$; $D(N_3O_7O_6O_4) = 42.64$
I-3	$R(N_3\cdots H_{13}-O_6) = 1.8092$; $A(N_3\cdots H_{13}-O_6) = 168.5$; $R(C_1-H_8\cdots O_7) = 2.7735$; $A(C_1-H_8\cdots O_7) = 115.1$; $D(C_1O_7O_6N_3) = -19.56$
I-4	$R(O_5\cdots H_{13}-O_6) = 1.9460$; $A(O_5\cdots H_{13}-O_6) = 169.6$; $R(C_1-H_8\cdots O_7) = 2.5057$; $A(C_1-H_8\cdots O_7) = 147.1$; $D(C_1O_7O_6O_5) = 31.09$
II-1	$R(O_4\cdots H_{13}-O_6) = 1.8752$; $A(O_4\cdots H_{13}-O_6) = 141.2$; $R(O_5-H_{12}\cdots O_6) = 1.8709$; $A(O_5-H_{12}\cdots O_6) = 153.3$; $D(O_4O_6O_5C_2) = -0.1107$
II-2	$R(O_5\cdots H_{13}-O_6) = 1.9420$; $A(O_5\cdots H_{13}-O_6) = 176.0$; $R(N_3-H_{11}\cdots O_7) = 2.2157$; $A(N_3-H_{11}\cdots O_7) = 159.4$; $D(N_3O_7O_6O_5) = 36.88$
II-3	$R(N_3\cdots H_{13}-O_6) = 1.8142$; $A(O_5\cdots H_{13}-O_6) = 168.6$; $R(C_1-H_8\cdots O_7) = 2.7794$; $A(C_1-H_8\cdots O_7) = 115.7$; $D(C_1O_7O_6N_3) = 19.87$
II-4	$R(O_4\cdots H_{13}-O_6) = 1.8416$; $A(O_4\cdots H_{13}-O_6) = 170.9$; $R(C_1-H_8\cdots O_7) = 2.4930$; $A(C_1-H_8\cdots O_7) = 141.2$; $D(C_1O_7O_6O_5) = -33.30$
III-1	$R(O_4\cdots H_{13}-O_6) = 1.8564$; $A(O_4\cdots H_{13}-O_6) = 177.3$; $D(O_6O_4C_2O_5) = -17.43$
III-2	$R(N_3\cdots H_{13}-O_6) = 1.7278$; $A(N_3\cdots H_{13}-O_6) = 157.2$; $R(O_5-H_{12}\cdots O_6) = 1.8017$; $A(O_5-H_{12}\cdots O_6) = 168.5$; $D(O_5O_6N_3C_1) = 40.61$
III-3	$R(O_5\cdots H_{13}-O_6) = 2.0019$; $A(O_5\cdots H_{13}-O_6) = 148.9$; $R(N_3-H_{11}\cdots O_7) = 2.4968$; $A(N_3-H_{11}\cdots O_7) = 123.6$; $D(N_3O_7O_6O_5) = -31.74$
III-4	$R(O_4\cdots H_{13}-O_6) = 1.7962$; $A(O_4\cdots H_{13}-O_6) = 170.0$; $R(C_1-H_8\cdots O_7) = 2.4340$; $A(C_1-H_8\cdots O_7) = 134.4$; $D(C_1O_7O_6O_4) = -37.39$

bonds in **I-3** and **II-3**. Namely, the elongations of the bonds O_6-H_{13} and C_1-N_3 (0.0254 and 0.0110 Å for **I-3**, 0.0247 and 0.0117 Å for **II-3**) and the very short $O_6-H_{13}\cdots N_3$ (1.8092 Å for **I-3**, 1.8142 Å for **II-3**) bond presumably lead to the longer $C_1-H_8\cdots O_7$ lengths. Of course, the strong proton affinity of the N atom should play a central role in strengthening the $O_6-H_{13}\cdots N_3$ bond. The shortening of C_1-H_8 in **I-3**, **I-4**, **II-4**, and **III-4** shows one of the fingerprint characteristics of improper $C-H\cdots Y$ hydrogen bonds.²⁸

In Table 2, the correlation between the angle and the length of the bond $C_1(N_3, O_{4,5})-H\cdots O$ does not show that their strength should be enhanced with the increase of HB linearity. This may be caused by the directional electrostatic interactions as far as dipole-dipole interactions between glycine and H_2O_2 . Table

3 shows the relative energies (δE) among the complexes as well as the free monomers for reference. The larger basis set 6-311++G(2df,2p) was used in the extrapolated calculations to determine the relative stability of the complexes. At the B3LYP/6-31++G(d,p) level, both δE and $\delta E+ZPVE$ (where the zero-point-vibrational-energy corrections were included without scaling) values indicate the same stability order. Moreover, the extrapolated calculations only predict the larger δE values (except for **I-2**) with respect to **I-1**, but do not alter this stability order. In general, complex **I-1** is the most stable one that has a dipole moment ($\mu = 1.27$ D) as small as the free monomer **I-0**. Four directional attacks to glycine by H_2O_2 may lead to larger or smaller dipole moments of the complexes with respect to the sum of dipole moments of the monomers, indicating the complexity of the electrostatic interactions.

On the basis of the NBO analyses (see details in section C), the binding energies ΔE of the complexes were decomposed into several terms summarized in Table 4. The ΔE_{CT} term can be closely tracked by $E(2)$ in eq 3, as proposed by Reed et al.²⁹ We found that the other smaller component of $E(2)$ cannot be omitted (see details in section C) if one wants to estimate the total CT effects. Thereby, the ΔE_{CT} terms were obtained by summarizing two components of $E(2)$ for $n_O \rightarrow \sigma^*_{X-H}$ in Table 6. In the NBO scheme, ΔE_{CT} is evaluated as the variational energy lowering due to expanding the variational space on each monomer to include unfilled orbitals on the other monomer, and its value is negative as shown in eq 3. Thereby, one can further calculate ΔE_{NCT} with eq 2. ΔE_{NCT} is due to exclusive repulsion and electrostatic (induction and polarization) interactions, and its value is positive as shown in Table 4. In addition, the preparation energy ΔE_{prep} is positive because the structural deformation brings the molecular energy to a higher energy level. In Table 4, the absolute values of ΔE_{CT} (−55.61 kcal/mol), ΔE_{NCT} (42.92 kcal/mol), and ΔE_{int} (−12.69 kcal/mol) of complex **III-2** are the largest, but the binding energy ΔE (−5.60 kcal/mol) is not the largest one, due to the highest ΔE_{prep} (7.08 kcal/mol) indicating the serious structural deformation to form this complex. ΔE_{int} is regarded as the hydrogen-bonding energy (E_{HB}) by other researchers. If hydrogen bonding is thought to stabilize the complex, the E_{HB} value should be the ΔE_{CT} in this work. In Table 4, the values of ΔE_{CT} are a little larger than the ΔE_{NCT} , because the hydrogen bonding is a short-distance force, while the electrostatic interaction is a long-distance force; namely, the former should be predominant as two monomers get together. Correlation between the relative energy with zero-point-vibration-energy correction ($\delta E+ZPVE$) and the binding

TABLE 3: Relative Energies (δE in kcal/mol) and Dipole Moments (μ in debye)

	I-0	II-0	III-0		H ₂ O ₂
δE	0.00	1.50	0.39	$E(+151 \text{ hatree})$	−0.558605
$\delta E + \text{ZPVE}^a$	0.00	1.50	0.08	$E + \text{ZPVE}(+151 \text{ hatree})^a$	−0.532164
μ	1.21	1.94	5.88	μ	1.79

	I-1	I-2	I-3	I-4	II-1	II-2	II-3	II-4	III-1	III-2	III-3	III-4
δE	0.00	1.92	0.15	5.37	1.08	6.19	1.98	4.06	3.15	3.11	3.24	0.89
δE^a	0.00	1.76	0.78	5.27	1.20	6.21	2.75	3.98	3.14	3.81	3.54	1.17
$\delta E + \text{ZPVE}^b$	0.00	1.79	0.19	4.74	1.12	5.84	2.02	3.80	2.92	3.65	3.47	1.07
μ	1.27	3.28	2.21	2.11	1.19	1.44	3.90	3.78	8.55	6.22	4.35	5.02

^a The B3LYP/6-311++G(2df,2p) over the B3LYP/6-31++G(d,p) optimized geometries. ^b Including zero-point-vibrational-energy (ZPVE) corrections.

TABLE 4: Preparation Energies (ΔE_{prep}), Charge-Transfer Energies (ΔE_{CT}), Non-Charge-Transfer Energies (ΔE_{NCT}), Interaction Energies (ΔE_{int}), and Bonding Energies (ΔE) of the Complexes, in kcal/mol

	ΔE_{prep}	ΔE_{CT}^a	ΔE_{NCT}^b	ΔE_{int}	ΔE
I-1	0.67	−25.59	15.97	−9.62	−8.95
I-2	0.42	−19.76	12.29	−7.47	−7.06
I-3	0.51	−27.26	18.16	−9.01	−8.60
I-4	0.21	−11.33	7.48	−3.85	−3.64
II-1	0.74	−31.04	20.94	−10.10	−9.36
II-2	0.39	−14.24	9.64	−4.60	−4.21
II-3	0.49	−26.74	17.97	−8.77	−8.28
II-4	0.28	−17.10	10.31	−6.79	−6.51
III-1	0.26	−14.56	7.82	−6.75	−6.48
III-2	7.08	−55.61	42.92	−12.69	−5.60
III-3	0.62	−8.69	2.06	−6.63	−6.00
III-4	0.47	−22.14	13.15	−8.99	−8.52

^a Sum of two components of $E(2)$ of the charge transfer for n_O; see discussion in the text. ^b $\Delta E_{\text{NCT}} = \Delta E_{\text{int}} - \Delta E_{\text{CT}}$.

energy ΔE is plotted in Figure 5. Each series of the complexes shows a perfect linearization,

$$-\Delta E \cong (\delta E + \text{ZPVE}) + \text{const.} \quad (4)$$

indicating that the binding energies play a central role in the relative stabilities for each series of complexes. The relative energies of the monomers or the other interaction components may also be important to determine the relative stabilities among different series of complexes.

B. Vibrational Frequencies. Significant frequency shifts were predicted for the O–H stretching and HOC out-of-plane wagging modes; they together with the frequency shifts of the C–H and N–H stretching modes were listed in Table 5. As the O–H group of the glycine or H₂O₂ moiety is involved in hydrogen bonding, the frequency shift will be many wavenumbers. The HOC out-of-plane wagging mode shows distinct blue-shifts for **I-1** (209.4 cm^{−1}), **II-1** (212.2 cm^{−1}), and **III-1** (34.3 cm^{−1}). This can be interpreted by the fact that the strong hydrogen bonding results in narrower HOC potential wells. However, the blue-shift for **III-3** (102.7 cm^{−1}) may be due to the deformation of the glycine plane and the intramolecular hydrogen-bonding effect. Red-shifts in the O–H stretching frequency have been traditionally considered one of the main fingerprints of HBs, assuming that formation of a HB weakens an O–H single bond. In fact, the large shifts appear in the O–H stretching frequencies of **I-3** (−498.6 cm^{−1}), **II-3** (−486.7 cm^{−1}), and **III-3** (−732.0 cm^{−1}), suggesting that the N atom is a remarkable proton acceptor. A perfect linear correlation ($r = 0.9993$) between the O–H bond elongation (ΔR) and the red-

shift ($-\Delta\omega$), except for **I-1**, **II-1**, and **III-3**, is shown in Figure 6a,

$$\Delta\omega(\text{cm}^{-1}) = 15.676 - 19.830\Delta R(\times 10^{-3}\text{\AA}) \quad (5)$$

On the basis of harmonic vibrational approximation, it is easy to understand this linear correlation if these frequencies represent the localized O–H stretching and almost do not depend on the proton acceptors.³⁰ However, the shifts will deviate from this linear correlation if these vibrations couple with the other groups (even with the other OH group). In Figure 6a, the points (◆) represent the red-shifts of the mixed O–H stretching in **I-1**, **II-1**, and **III-3**.

In complexes **I-1** and **II-1**, the strong RAHB mechanism can lead to the mixed O–H stretching modes in which the symmetric (s) O₅–H₁₂ and O₆–H₁₃ stretching is 3433.1 cm^{−1} for **I-1** and 3413.2 cm^{−1} for **II-1**; the asymmetric (a) stretching is 3517.6 cm^{−1} for **I-1** and 3498.7 cm^{−1} for **II-1**. Moreover, for **I-1**, the small contribution of the symmetric NH₂ stretching is found in the asymmetric mixed O–H stretching frequency 3517.6 cm^{−1}; in fact, the symmetric NH₂ stretching (3519.0 cm^{−1}) also shows some characteristics of the O₅–H₁₂ and O₆–H₁₃ stretching. This mixing may be due to a Fermi resonance because the free symmetric NH₂ stretching frequency is predicted to be 3517.8 cm^{−1} at the same level of theory. However, this phenomenon is not observed for **II-1**, since the free NH₂ stretching frequencies of the free monomer **II-0** are predicted to be 3525.9 cm^{−1} (symmetric) and 3610.4 cm^{−1} (asymmetric), which are much larger than the mixed O–H stretching frequencies. The other mixed stretching modes are also found in **III-2** and **III-3**.

The frequency shifts for the CH₂ and NH₂ stretching are not simply understood as the case of a single bond O–H stretching in the above discussion. First, the bond involved in the hydrogen bond may be shortened (−0.6 mÅ of C₁–H₈ in **I-4**), while the other that is not in the hydrogen bond may be elongated (0.7 mÅ of C₁–H₉ in **I-4**) or shortened (−1.4 mÅ of C₁–H₉ in **I-3**). The former corresponds to a red-shift (−1.2 cm^{−1}), but the latter is a blue-shift (6.2 cm^{−1}) for **I-4**. Only red-shifts (−19.7 and −8.7 cm^{−1}) were predicted for the NH₂ stretching in **III-3**; the corresponding ones in the other complexes are blue-shifts (see Table 5). As pointed out by Hobza and Havlas,²⁸ the *improper* hydrogen bonding may lead to a shortening of the X–H (X = C in ref 28) due to the relaxation of the charge-accepting monomer. To study whether these *improper* HBs have a similar correlation between frequency shift and the bond length change (despite elongating or shortening), the algebraic sums of two bond length changes (C₁–H₈ and C₁–H₉ of **I-3**, **I-4**, **II-3**, **II-4**, **III-4**; or N₃–H₁₀ and N₃–H₁₁ of **I-2**, **II-2**, **III-3**) were calculated. It is interesting that the sums were found to correlate well with the algebraic sums of the respective frequency shifts

TABLE 5: Harmonic Frequencies (in cm^{-1}) and Intensities (in km/mol) for Some Selected Vibrational Modes

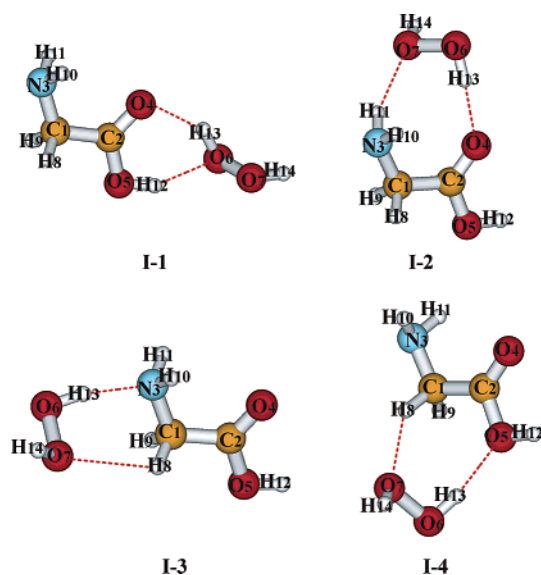
	HOC out-of-plane wagging mode		stretching mode OH in H_2O_2 moiety (involving hydrogen bond)		stretching mode OH in glycine moiety		CH stretching mode		NH stretching mode	
	freq ^a	int ^b	freq ^a	int ^b	freq ^a	int ^b	freq ^a	int ^b	freq ^a	int ^b
I-0	655.4	105.6	3766.6a ^c 3767.2s ^c	60.0 ^c 11.2 ^c	3747.3	56.5	3054.0s 3092.4a	17.0 6.5	3517.8s 3598.5a	1.5 5.9
I-1	864.8(209.4)	113.7(1.1)	3517.6(−249.3) ^d	567.3(15.9) ^d	3433.1(−314.2) ^d	204.8(3.6) ^d	3055.0(1.0)s 3093.2(0.8)a	17.0(1.0) 5.5(0.8)	3519.0(1.2) ^d s 3599.8(1.3)a	313.8(209.2) ^d 5.6(0.9)
I-2	661.7(6.3)	66.0(0.6)	3559.4(−207.5)	612.9(17.2)	3743.5(−3.8)	60.1(1.1)	3046.5(−7.5)s 3086.5(−5.9)a	18.5(1.1) 6.4(1.0)	3519.3(1.5)s 3609.8(11.3)a	10.3(6.9) 58.2(9.9)
I-3	654.4(−1.0)	98.1(0.9)	3268.3(−498.6)	1116.1(31.4)	3751.5(4.2)	68.1(1.2)	3073.2(19.2)s 3113.4(21.0)a	13.1(0.8) 1.7(0.3)	3508.2(−9.6)s 3583.2(−15.3)a	3.4(2.3) 12.7(2.2)
I-4	654.2(−1.2)	143.0(1.4)	3661.7(−105.2)	358.4(10.1)	3745.1(−2.2)	61.7(1.1)	3052.8(−1.2)s 3098.6(6.2)a	10.1(0.6) 2.1(0.3)	3521.3(3.5)s 3604.4(5.9)a	1.8(1.2) 6.2(1.1)
II-0	682.9	117.8			3752.1	65.8	3060.9s 3099.6a	16.1 5.1	3525.9s 3610.4a	1.8 6.0
II-1	895.1(212.2)	102.5(0.9)	3498.7(−268.2) ^e	960.0(27.0) ^e	3413.2(−338.9) ^e	184.0(2.8) ^e	3059.5(−1.4)s 3097.9(−1.7)a	16.2(1.0) 4.8(0.9)	3524.8(−1.1)s 3608.2(−2.2)a	3.6(2.0) 6.1(1.0)
II-2	694.6(11.7)	158.6(1.3)	3649.2(−117.7)	412.8(11.6)	3737.9(−14.2)	72.6(1.1)	3054.0(−6.9)s 3093.5(−6.2)a	19.0(1.2) 4.2(0.8)	3531.1(5.2)s 3625.5(15.1)a	25.8(14.3) 16.4(2.7)
II-3	681.4(−1.5)	107.4(0.9)	3280.2(−486.7)	1106.3(31.1)	3752.1(0.0)	75.0(1.1)	3076.4(15.5)s 3121.0(21.4)a	12.9(0.8) 1.3(0.3)	3514.6(−11.3)s 3594.0(−6.4)a	3.7(2.1) 12.6(2.1)
II-4	693.5(10.6)	154.2(1.3)	3545.8(−221.1)	602.7(16.9)	3745.1(−7.0)	72.6(1.1)	3054.5(6.4)s 3106.7(7.1)a	9.7(0.6) 1.7(0.3)	3529.3(3.4)s 3616.5(6.1)a	5.9(3.3) 6.6(1.1)
III-0	869.9	104.0			3464.5	293.3	3069.1s 3117.0a	13.0 5.4	3544.7s 3632.5a	0.3 18.0
III-1	904.2(34.3)	91.1(0.9)	3567.1(−199.8)	665.2(18.7)	3410.4(−54.1)	382.0(1.3)	3074.3(5.2)s 3122.2(5.2)a	9.1(0.7) 2.8(0.5)	3549.1(4.4)s 3636.1(2.6)a	2.4(22.3) 22.3(1.2)
III-2	823.9(−46.0)	96.1(0.9)	3034.9(−732.0)	854.1(24.0)	3441.9(−22.6) ^f	991.8(3.4) ^f	3061.7(−7.4)s ^f 3112.9(−4.1)a	74.9(5.8) ^f 10.9(2.0)	3494.39(−49.8)s 3575.0(−57.5)a	2.4(12.3) 12.6(0.7)
III-3	972.6(102.7)	98.7(0.9)	3628.4(−138.5) ^g	233.9(6.6) ^g	3370.6(−93.9)	320.2(1.1)	3061.1(−8.0)s 3107.5(−9.5)a	15.2(1.2) 7.4(1.4)	3525.0(−19.7)s 3623.8(−8.7)a ^g	9.7(7.8) 7.8(0.4) ^g
III-4	922.5(52.6)	31.0(0.3)	3458.5(−308.4)	683.7(19.2)	3384.8(−79.7)	369.5(1.3)	3077.4(8.3)s 3126.1(9.1)a	2.9(0.2) 2.8(0.5)	3547.1(2.4)s 3633.0(0.5)a	2.3(20.9) 20.9(1.2)

^a Numbers in parentheses are frequency shifts relative to free monomers. ^b Numbers in parentheses are the ratios between the intensity of the complex and that in the monomer. ^c Of free H_2O_2 , using the average values of frequency and intensity to calculate the shifts and ratios. ^d Strong mixing modes including OH(H_2O_2), OH(glycine), and NH symmetric (s) stretching. ^e The mixing modes of OH(H_2O_2) and OH(glycine) stretching. ^f The mixing modes of OH(glycine) and CH symmetric (s) stretching. ^g The mixing modes of OH(H_2O_2) and NH asymmetric (a) stretching.

TABLE 6: Natural Bond Orbital Analysis of Intermolecular Hydrogen Bonds

		$E(2)^a$ (kcal/mol)	$\delta\epsilon^a$ (au)	F_{ij}^a (au)
I-1	$n_{O4} \rightarrow \sigma^*_{O6H13}$	10.07(3.93)	0.71(1.14)	0.078(0.060)
	$n_{O6} \rightarrow \sigma^*_{O5H12}$	15.18(0.41)	0.84(1.06)	0.101(0.019)
I-2	$n_{O4} \rightarrow \sigma^*_{O6H13}$	8.18(7.47)	0.77(1.19)	0.073(0.084)
	$n_{O7} \rightarrow \sigma^*_{N3H11}$	3.84(0.27)	1.09(0.98)	0.058(0.015)
I-3	$n_{N3} \rightarrow \sigma^*_{O6H13}$	26.94 ^b	0.78 ^b	0.131 ^b
	$n_{O7} \rightarrow \sigma^*_{C1H8}$	0.19(0.13)	0.76(1.14)	0.011(0.011)
I-4	$n_{O5} \rightarrow \sigma^*_{O6H13}$	8.13(1.59)	1.11(0.82)	0.085(0.033)
	$n_{O7} \rightarrow \sigma^*_{C1H8}$	0.98(0.63)	0.87(1.09)	0.026(0.023)
II-1	$n_{O4} \rightarrow \sigma^*_{O6H13}$	10.57(4.29)	0.70(1.13)	0.079(0.062)
	$n_{O6} \rightarrow \sigma^*_{O5H12}$	15.77(0.41)	0.83(1.06)	0.102(0.019)
II-2	$n_{O5} \rightarrow \sigma^*_{O6H13}$	7.80(2.36)	1.10(0.82)	0.083(0.041)
	$n_{O7} \rightarrow \sigma^*_{N3H11}$	3.70(0.38)	1.06(1.03)	0.056(0.018)
II-3	$n_{N3} \rightarrow \sigma^*_{O6H13}$	26.43 ^b	0.78 ^b	0.130 ^b
	$n_{O7} \rightarrow \sigma^*_{C1H8}$	0.18(0.13)	0.76(1.14)	0.010(0.011)
II-4	$n_{O4} \rightarrow \sigma^*_{O6H13}$	10.68(5.62)	0.77(1.19)	0.084(0.073)
	$n_{O7} \rightarrow \sigma^*_{C1H8}$	1.28(0.40)	0.90(1.04)	0.030(0.018)
III-1	$n_{O4} \rightarrow \sigma^*_{O6H13}$	8.17(6.39)	0.77(1.20)	0.073(0.078)
	$n_{N3} \rightarrow \sigma^*_{O6H13}$	35.97 ^b	0.74 ^b	0.147 ^b
III-2	$n_{O6} \rightarrow \sigma^*_{O5H12}$	19.08(0.56)	0.83(1.08)	0.112(0.022)
	$n_{O5} \rightarrow \sigma^*_{O6H13}$	5.52(2.44)	0.79(1.07)	0.062(0.046)
III-3	$n_{O7} \rightarrow \sigma^*_{N3H11}$	0.66(0.07)	1.20(0.82)	0.025(0.007)
	$n_{O4} \rightarrow \sigma^*_{O6H13}$	14.27(5.97)	0.75(1.16)	0.095(0.074)
III-4	$n_{O7} \rightarrow \sigma^*_{C1H8}$	1.59(0.31)	0.94(0.98)	0.035(0.015)

^a The values are O sp hybrid branch to form the hydrogen bond; those in the parentheses are O p hybrid branch. See discussion in the text. ^b The lone pair of N atom is mainly of p character.

**Figure 2.** Complexes **I-1**, **I-2**, **I-3**, and **I-4**.

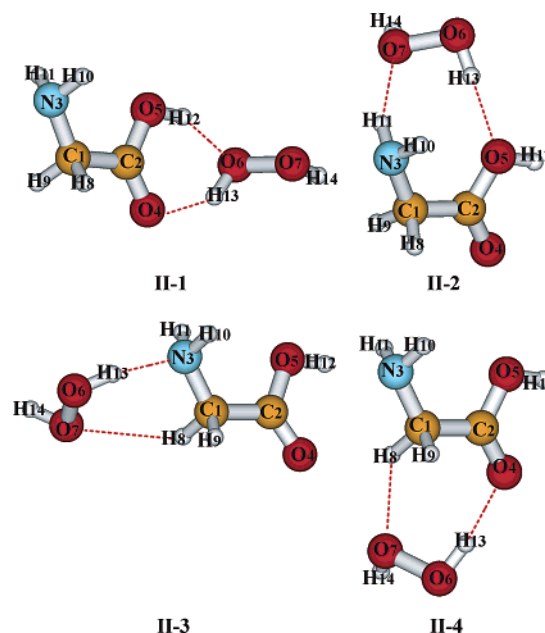
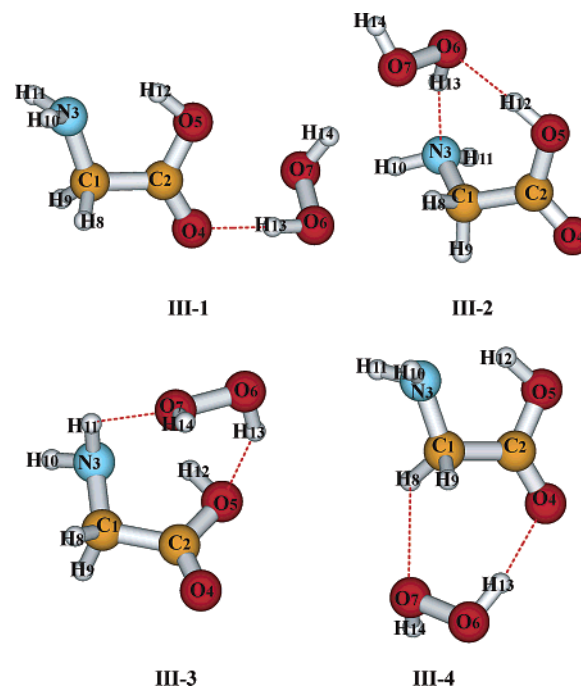
(symmetric and asymmetric). In Figure 6b, similar correlations were also fitted,

$$\Delta\omega(\text{cm}^{-1}) = 11.900 - 10.898\Delta R(\times 10^{-3} \text{ \AA}) \quad (6)$$

for the CH₂ stretching ($r = 0.9609$), and

$$\Delta\omega(\text{cm}^{-1}) = 3.856 - 12.136\Delta R(\times 10^{-3} \text{ \AA}) \quad (7)$$

for the NH₂ stretching ($r = 0.9996$). The constants in eqs 5–7 depend on the free X–H (X = O, C, N) characteristics. Here it is noted that no critical symmetric or asymmetric XH₂ (X = C, N) stretching modes exist in the complexes and monomers except for **I-0** and free H₂O₂ because of the low C₁ symmetry. We still labeled them according to the stretching phase. In the hydrogen-bonding complexes, one bond may be elongated significantly while the other may be shortened with a big margin

**Figure 3.** Complexes **II-1**, **II-2**, **II-3**, and **II-4**.**Figure 4.** Complexes **III-1**, **III-2**, **III-3**, and **III-4**.

(e.g., $\Delta R(\text{C}_1\text{--H}_8) = -1.2 \text{ m\AA}$ and $\Delta R(\text{C}_1\text{--H}_9) = 1.6 \text{ m\AA}$ of **II-4**). In one stretching mode, the contribution of an O–H stretching component is not equal to another. More seriously unequal CH₂ stretching modes are found in **II-4**: the C₁–H₉ stretching component is stronger in the symmetric vibration (3054.5 cm^{−1}), while the C₁–H₈ stretching component is stronger in the asymmetric vibration (3106.7 cm^{−1}). The equal contributions were used in Figure 6b; this approximation leads to the lower two points away from the fitted line for the CH₂ stretching. Only three points for the NH₂ stretching were given. However, the consistency of the correlation between the bond length change and frequency shift has been found in Figure 6, without reference to the weak and strong HBs or to the blue- and red-shifts. This further suggests that the *improper* HBs²⁸ should be *proper*.

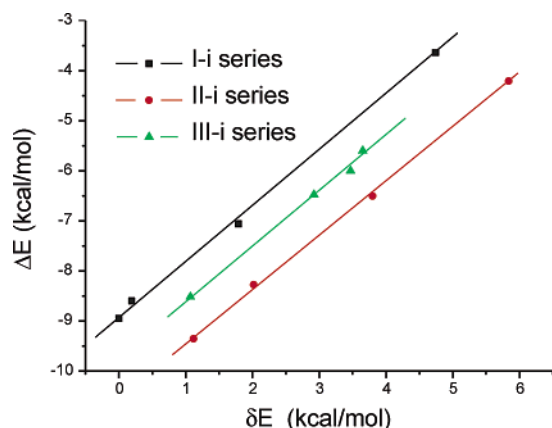


Figure 5. Correlation between the relative stability δE and the binding energy ΔE .

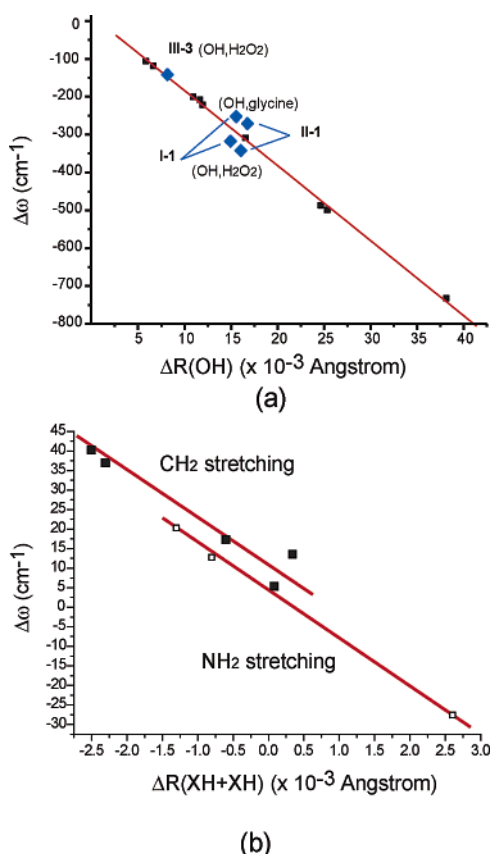


Figure 6. (a) Correlation between the frequency shifts $\Delta\omega$ and the bond elongation $\Delta R(\text{O}-\text{H})$. (b) Correlation between the algebraic sum of the frequency shifts $\Delta\omega$ and the algebraic sum of the bond changes $\Delta R(\text{X}-\text{H})$ ($\text{X} = \text{C}, \text{N}$).

C. NBO and Topological Analysis. The NBO analysis originated as a technique for studying hybridization and covalency effects in polyatomic wave functions.¹⁹ In this work, the O atom involved in the hydrogen bonding has two branches: one has sp hybrid characteristics, and the other one has more p hybrid characteristics; they corresponds to two $E(2)$ values, respectively, as shown in Table 6. Although $E(2)$ depends on both $\delta\epsilon$ and F_{ij} in eq 3, the larger of the two $E(2)$ values always has sp characteristics for the O atoms. In contrast to the O atoms, the N₃ atom shows p characteristics in hydrogen bonding. Thereby, the O atoms exhibit more flexibility (less anisotropic) than the N atom in hydrogen bonding. Namely, the more nonlinear HB ($\text{A}(\text{N}_3\cdots\text{H}_{13}-\text{O}_6) = 157.2^\circ$, $R(\text{N}_3\cdots\text{H}_{13}-\text{O}_6) = 1.7278 \text{ \AA}$) in complex **III-2** is the strongest,

TABLE 7: Topological Properties of the Bond Critical Points of the Intramolecular Hydrogen Bonds and Natural Charge Transfer between Glycine and H_2O_2 in the Complexes

		ρ (au)	$\nabla^2\rho$ (au)	charge transfer ^a (10^{-3}e)
I-1	$\text{O}_5-\text{H}_{12}\cdots\text{O}_6$	0.0311	0.0855	−5.04
	$\text{O}_6-\text{H}_{13}\cdots\text{O}_4$	0.0309	0.0868	
	ring($\text{C}_2\text{O}_4\text{H}_{13}\text{O}_6\text{H}_{12}\text{O}_5$)	0.0131		
I-2	$\text{N}_3-\text{H}_{11}\cdots\text{O}_7$	0.0145	0.0467	18.81
	$\text{O}_6-\text{H}_{13}\cdots\text{O}_4$	0.0301	0.0928	
I-3	$\text{O}_6-\text{H}_{13}\cdots\text{N}_3$	0.0426	0.0936	59.01
	$\text{C}_1-\text{H}_8\cdots\text{O}_7$	0.0053	0.0215	
	ring($\text{C}_1\text{N}_3\text{H}_{13}\text{O}_6\text{O}_7\text{H}_8$)	0.0051		
I-4	$\text{O}_6-\text{H}_{13}\cdots\text{O}_5$	0.0243	0.0706	12.17
	$\text{C}_1-\text{H}_8\cdots\text{O}_7$	0.0082	0.0289	
	ring($\text{C}_1\text{H}_8\text{O}_7\text{O}_6\text{H}_{13}\text{O}_5\text{C}_2$)	0.0037		
		0.0037		
II-1	$\text{O}_5-\text{H}_{12}\cdots\text{O}_6$	0.0319	0.0879	−3.88
	$\text{O}_6-\text{H}_{13}\cdots\text{O}_4$	0.0318	0.0893	
	ring($\text{C}_2\text{O}_4\text{H}_{13}\text{O}_6\text{H}_{12}\text{O}_5$)	0.0134		
II-2	$\text{N}_3-\text{H}_{11}\cdots\text{O}_7$	0.0094	0.0389	9.84
	$\text{O}_6-\text{H}_{13}\cdots\text{O}_5$	0.0241	0.0697	
II-3	$\text{O}_6-\text{H}_{13}\cdots\text{N}_3$	0.0422	0.0929	57.80
	$\text{C}_1-\text{H}_8\cdots\text{O}_7$	0.0052	0.0211	
	ring($\text{C}_1\text{N}_3\text{H}_{13}\text{O}_6\text{O}_7\text{H}_8$)	0.0050		
II-4	$\text{O}_6-\text{H}_{13}\cdots\text{O}_4$	0.0312	0.0912	24.93
	$\text{C}_1-\text{H}_8\cdots\text{O}_7$	0.0086	0.0301	
	ring($\text{C}_1\text{H}_8\text{O}_7\text{O}_6\text{H}_{13}\text{O}_4\text{C}_2$)	0.0043		
III-1	$\text{O}_6-\text{H}_{13}\cdots\text{O}_4$	0.0295	0.0874	28.00
	$\text{O}_5-\text{H}_{12}\cdots\text{O}_6$	0.0362	0.0998	
III-2	$\text{O}_6-\text{H}_{13}\cdots\text{N}_3$	0.0527	0.106	33.78
	$\text{O}_6-\text{H}_{13}\cdots\text{O}_5$	0.0230	0.0644	
III-3	$\text{N}_3-\text{H}_{11}\cdots\text{O}_7$	0.0083	0.0326	9.66
	$\text{O}_6-\text{H}_{13}\cdots\text{O}_4$	0.0354	0.102	
III-4	$\text{C}_1-\text{H}_8\cdots\text{O}_7$	0.0099	0.0341	32.70
	ring($\text{C}_1\text{H}_8\text{O}_7\text{O}_6\text{H}_{13}\text{O}_4\text{C}_2$)	0.0047		

^a The total charge transfer from glycine to H_2O_2 with the positive sign for the glycine moiety; otherwise the negative value shows the reverse transfer.

accompanied by the largest $E(2)$ value of 35.97 kcal/mol. The other $E(2)$ values for $\text{n}_\text{O} \rightarrow \sigma^*_{\text{OH}}$ are small (5.52–19.08 kcal/mol), and those for $\text{n}_\text{O} \rightarrow \sigma^*_{\text{CH}}$ and $\text{n}_\text{O} \rightarrow \sigma^*_{\text{NH}}$ are smaller (0.18–3.84 kcal/mol). Moreover, the weak CT processes, $\text{n}_\text{O} \rightarrow \sigma^*_{\text{CH}}$ and $\text{n}_\text{O} \rightarrow \sigma^*_{\text{NH}}$, seem to predominately depend on the F_{ij} values.

On the other hand, since the DFT (in particular, B3LYP) densities compared with MP2 densities have been demonstrated to be valid to model hydrogen-bonding crystal systems^{31a} and complexes,^{31b} the topological features of electron densities of the glycine– H_2O_2 complexes were predicted at the B3LYP/6-31++G(d,p) level of theory and the AIM theory. In the AIM theory, three criteria to distinguish the hydrogen bonding from other interactions have been suggested: (i) the existence of a bond critical point (BCP) as well as a ring critical point (RCP) in the hydrogen-bonding path, (ii) a value of electron density ρ at the BCP or RCP in the range of 0.002–0.04 au, and (iii) a positive $\nabla^2\rho$ in the range 0.02–0.15 au.³² The calculated topological properties have been summarized in Table 7. The strongest HB, $\text{O}-\text{H}\cdots\text{N}$, has the largest densities, $\rho = 0.0422$ –0.0527 au; the stronger HB, $\text{O}-\text{H}\cdots\text{O}$, has the larger densities, $\rho = 0.0230$ –0.0362 au; and the weak HBs, $\text{C}-\text{H}\cdots\text{O}$ and $\text{N}-\text{H}\cdots\text{O}$, have the smallest densities, $\rho = 0.0052$ –0.0145 au. Several RCPs have been found in these complexes, in which the six-membered rings have the larger densities, $\rho = 0.0131$ au in **I-1** and $\rho = 0.0134$ au in **II-2**. This indicates the existence of cooperative effects in these two complexes. The RCPs in complexes **I-1** and **II-2** are also consistent with the RAHB mechanism discussed above. Both cooperative effects and

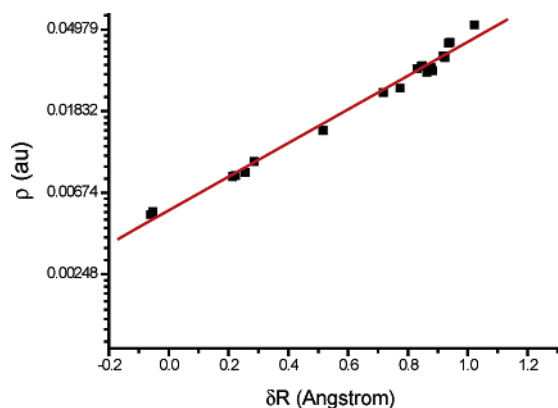


Figure 7. Correlation between the electron density ρ at the bond critical points in the logarithmic value ($\ln \rho$) and the hydrogen bond parameter δR .

RAHB enhance the strength of O–H···O, while O₁₃–H₁₃···O₄ is much weaker ($\rho = 0.0295$ au) in **III-1** because of the nonexistence of the cooperative effect and RAHB mechanism. Moreover, the CT analyses based on the NBO calculations show that only in **I-1** and **II-1** does the glycine moiety attract the electronic charge from the H₂O₂. This is also suspected to be related to the cooperative effects and RAHB mechanism.

To understand the nature of HB with the density properties at the BCPs, the quantity of evidence shows that the short HB has the largest ρ .³³ As pointed out by Galvez et al.,^{31b} the linear behavior between the density and the HB length is only held in the neighborhood of equilibrium, while the density ρ decays exponentially in the long range. Here we use another HB parameter, δR , defined as

$$\delta R = R_{\text{H}}^{\text{vdW}} + R_{\text{Y}}^{\text{vdW}} - R_{\text{H}\cdots\text{Y}} \quad (8)$$

where $R_{\text{H}}^{\text{vdW}}$ and $R_{\text{Y}}^{\text{vdW}}$ are the van der Waals radii of H and Y atoms, respectively. $R_{\text{H}\cdots\text{Y}}$ is the length of the HB(H···Y). The logarithmic plot $\ln \rho \approx \delta R$ is shown in Figure 7, where the van der Waals radii were given by Bondi.³⁴ The fitted exponential correlation ($r = 0.9943$) is

$$\ln \rho(\text{au}) = -5.217 + 2.067 \delta R (\times 10^{-3} \text{ \AA}) \quad (9)$$

For the extremely weak HBs, C–H···O in **I-3** and **II-3**, the δR values are negative, indicating the distance between the O and H atoms is longer than the sum of their van der Waals radii. This suggests that eq 9 should be able to describe a wide range of intermolecular interactions.

Furthermore, the other two ρ -related correlations were plotted in Figure 8a, $F_{ij} \approx \rho$, and in Figure 8b, $-\Delta E_{\text{int}} \approx \rho_{\text{tot}}$, respectively. Here the F_{ij} matrix is the larger one and the densities ρ are obtained with the AIM theory; ρ_{tot} is the sum of the densities at BCPs and RCPs. Through Mulliken-type approximations,³⁵ the Fock matrix can be

$$F_{ij} = \langle \sigma | F | \sigma^* \rangle \approx k \langle \sigma | \sigma^* \rangle \quad (10)$$

This pre-natural-atomic-orbital overlap integral seems to be proportional to the occupied MO overlap (to calculate ρ) in AIM, $F_{ij} \approx 2.804\rho$ ($r = 0.9743$), which is shown in Figure 8a. The interaction energies of the complexes linearly depend on the total densities ($r = 0.9011$), as shown in Figure 8b,

$$\Delta E_{\text{int}}(\text{kcal/mol}) \cong -126.976\rho_{\text{tot}}(\text{au}) - 1.974 \quad (11)$$

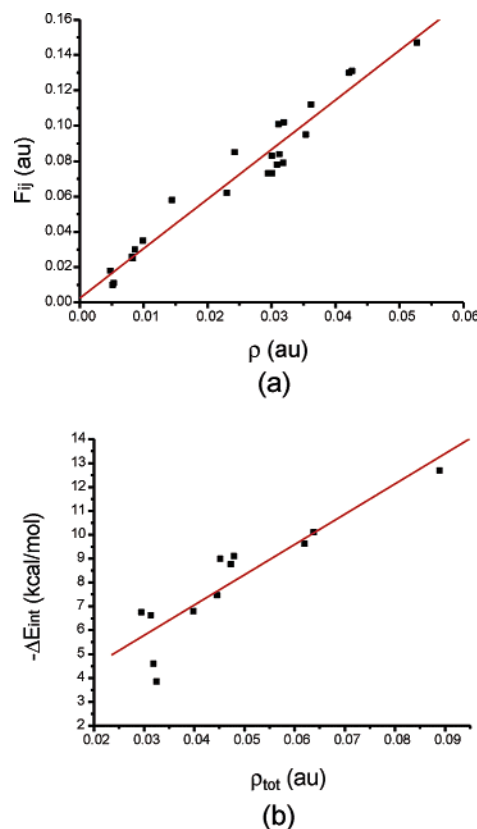


Figure 8. (a) Correlation between the Fock matrix element F_{ij} (the sp branch for the O atom) and the electron density ρ at the bond critical points. (b) Correlation between the interaction energy ΔE_{int} and the total electron densities ρ_{tot} at the critical points of the complex.

In general, the larger densities at the critical points lead to stronger interactions besides the hydrogen bonding.

4. Concluding Remarks

The DFT-B3LYP/6-31++G(d,p) level of theory, NBO, and AIM analysis have been employed to study glycine–H₂O₂ complexes. Several structural, energetic, and vibrational features are predicted: (a) These complexes are doubly hydrogen bonding except for **III-3**; (b) for the most stable glycine isomers, the energetically favorable isomer attacks by H₂O₂ to form the hydrogen bonds at the COOH and NH₂–CH₂ sides in **I-0** and **II-0** and the C=O–CH₂ side in **III-0**; (c) significant frequency red-shifts for the O–H stretching (-105.2 to -732.0 cm⁻¹) are predicted; some mixing vibrations are interpreted by the following mechanisms; (d) the distinguished cooperative effects and the typical resonance-assisted hydrogen bonding are found in the six-membered rings of complexes **I-1** and **II-1**; (e) the binding energies play a central role in the relative stabilities of the complexes, among which complex **I-1** is the most stable conformer. Moreover, a strength sequence of the hydrogen bonds from the strongest to the weakest is O–H···N, O–H···O, N–H···O, and C–H···O. The change of the bond length linearly correlates with the corresponding frequency shift, without reference to the hydrogen-bonding strength or type. The NBO analyses show that the charge transfers from glycine to H₂O₂ in these complexes except for **I-1** and **II-1**. The electron density ρ at the critical points predicted by the AIM theory significantly correlates with the hydrogen-bonding parameter $\delta R_{\text{H}\cdots\text{Y}}$, the Fock matrix element F_{ij} , and the interaction energy of the complex.

References and Notes

- (1) Glass, W. A.; Varma, M. N., Eds. *Physical and Chemical Mechanism in Molecular Radiation Biology*; Plenum Press: New York, 1991.
- (2) Varma, S. D.; Devamanoharan, P. S. *Free Radical Res. Commun.* **1991**, *14*, 125.
- (3) Dizdaroğlu, M.; Nackerdien, Z.; Chao, B. C.; Gajewski, E.; Rao, G. *Arch. Biochem. Biophys.* **1991**, *285*, 388.
- (4) Gould, I. R.; Kollman, P. A. *J. Am. Chem. Soc.* **1994**, *116*, 2493.
- (5) Schoone, K.; Smets, J.; Houben, L.; Vanbael, M. K.; Adamowicz, L.; Maes, G. *J. Phys. Chem. A* **1998**, *102*, 4863.
- (6) Dobado, J. A.; Molina, J. *J. Phys. Chem. A* **1999**, *103*, 4755.
- (7) Wysokiński, R.; Michalska, D.; Bieńko, D. C.; Zeegers-Huyskens, T. *J. Phys. Chem. A* **2003**, *107*, 8730.
- (8) Serra, M. A.; Dörner, B. K.; Silver, M. E. *Acta Crystallogr. C* **1992**, *48*, 1957.
- (9) (a) Dobado, J. A.; Molina, J. *J. Phys. Chem.* **1993**, *97*, 7499. (b) Mo, O.; Yañez, M.; Rozas, I.; Elguero, J. *J. Chem. Phys.* **1994**, *100*, 2871. (c) Dobado, J. A.; Molina, J. *J. Phys. Chem.* **1994**, *98*, 1819. (d) Dobado, J. A.; Molina, J. *J. Phys. Chem.* **1994**, *98*, 7819. (e) Dobado, J. A.; Molina, J.; Portal, D. *J. Phys. Chem. A* **1998**, *102*, 778.
- (10) (a) Berger, P.; Vel Leitner, K. N.; Doré, M.; Legube, B. *Water Res.* **1999**, *33*, 433, and references therein. (b) Galano, A.; Alvarez-Idaboy, J. R.; Montero, L. A.; Vivier-Bunge, A. *J. Comput. Chem.* **2001**, *22*, 1138.
- (11) Duguet, J. P.; Brodard, E.; Dussert, B.; Mallevalle, J. *Ozone Sci. Eng.* **1985**, *7*, 105.
- (12) (a) Schubert, J.; Wilmer, J. W. *Free Radical Biol. Med.* **1991**, *11*, 545. (b) Alvarez-Idaboy, J. R.; Mora-Diez, N.; Boyd, R. J.; Vivier-Bunge, A. *J. Am. Chem. Soc.* **2001**, *123*, 2018. (c) Smith, I. W. M.; Ravishankara, A. R. *J. Phys. Chem. A* **2002**, *92*, 5347.
- (13) (a) Jeffrey, G. A. *An Introduction to Hydrogen Bonding*; Oxford University Press: New York, 1997. (b) Desiraju, G. R.; Steiner, T. *The Weak Hydrogen Bond in Structural Chemistry and Biology*; Oxford University Press: New York, 1999.
- (14) Steiner, T. *Angew. Chem., Int. Ed.* **2002**, *41*, 48.
- (15) Guerra, C. F.; Bickelhaupt, F. M.; Snijders, E. J. *J. Am. Chem. Soc.* **2000**, *122*, 4117, and references therein.
- (16) For examples: (a) Brustolon M.; Chis, V.; Maniero, A. L.; Brunel, L.-C. *J. Phys. Chem. A* **1997**, *101*, 4887. (b) Rega, N.; Cossi, M.; Barone, V. *J. Am. Chem. Soc.* **1997**, *119*, 12962. (c) Gutowski, M.; Skurski, P.; Simons, J. *J. Am. Chem. Soc.* **2000**, *122*, 10159. (d) Bonifacic, M.; Stefanic, I.; Hug, G. L.; Armstrong, D. A.; Asmus, K.-D. *J. Am. Chem. Soc.* **1998**, *120*, 9930. (e) Yu, D.; Rauk, A.; Armstrong, D. A. *J. Am. Chem. Soc.* **1995**, *117*, 1789.
- (17) (a) Perutz, M. F.; Fermi, G.; Abraham, D. J.; Poyart, C.; Bursaux, E. *J. Am. Chem. Soc.* **1986**, *108*, 1064. (b) Engh, R. A.; Brandstetter, H.; Sucher, G.; Eichinger, A.; Baumann, I.; Bode, W. *Structure* **1996**, *4*, 1353.
- (18) (a) Morokuma, K. *Chem. Phys.* **1971**, *55*, 1236. (b) Kitaura, K.; Morokuma, K. *Int. J. Quantum Chem.* **1976**, *10*, 325.
- (19) Reed, A.; Curtiss, L. A.; Weinhold, F. *Chem. Rev.* **1988**, *88*, 899.
- (20) (a) Becke, A. D. *J. Chem. Phys.* **1993**, *98*, 5648. (b) Lee, C. T.; Yang, W.; Parr, R. G. *Phys. Rev. B* **1988**, *37*, 785.
- (21) Frisch, M. J.; Trucks, G. W.; Schlegel, H. B.; Scuseria, G. E.; Robb, M. A.; Cheeseman, J. R.; Zakrzewski, V. G.; Montgomery, J. A., Jr.; Stratmann, R. E.; Burant, J. C.; Dapprich, S.; Millam, J. M.; Daniels, A. D.; Kudin, K. N.; Strain, M. C.; Farkas, O.; Tomasi, J.; Barone, V.; Cossi, M.; Cammi, R.; Mennucci, B.; Pomelli, C.; Adamo, C.; Clifford, S.; Ochterski, J.; Petersson, G. A.; Ayala, P. Y.; Cui, Q.; Morokuma, K.; Malick, D. K.; Rabuck, A. D.; Raghavachari, K.; Foresman, J. B.; Cioslowski, J.; Ortiz, J. V.; Baboul, A. G.; Stefanov, B. B.; Liu, G.; Liashenko, A.; Piskorz, P.; Komaromi, I.; Gomperts, R.; Martin, R. L.; Fox, D. J.; Keith, T.; Al-Laham, M. A.; Peng, C. Y.; Nanayakkara, A.; Gonzalez, C.; Challacombe, M.; Gill, P. M. W.; Johnson, B.; Chen, W.; Wong, M. W.; Andres, J. L.; Gonzalez, C.; Head-Gordon, M.; Replogle, E. S.; Pople, J. A. *GAUSSIAN 98*; Gaussian, Inc.: Pittsburgh, PA, 1998.
- (22) (a) Chandra, A. K.; Nguyen, M. T.; Zeegers-Huyskens, T. *J. Chem. Soc., Faraday Trans.* **1998**, *94*, 1277. (b) Hocquet, A.; Leulliot, N.; Ghomi, M. *J. Phys. Chem. B* **2000**, *104*, 10934. (c) Gaigeot, M. P.; Leulliot, N.; Ghomi, M.; Jobic, H.; Bouloussa, O.; Coulombeau, C. *Chem. Phys.* **2000**, *261*, 217. (d) Simon, S.; Sodupe, M.; Bertain, J. *J. Phys. Chem. A* **2002**, *106*, 5397. (e) Bertain, J.; Rodriguez-Santiago, L.; Bodupe, M. *J. Phys. Chem. B* **1999**, *103*, 2310.
- (23) Kurinovich, M. A.; Lee, J. K. *J. Am. Chem. Soc.* **2000**, *122*, 6258.
- (24) Boys, S. F.; Bernardi, F. *Mol. Phys.* **1970**, *19*, 553.
- (25) Glendening, E. D.; Reed, A. E.; Carpenter, J. E.; Weinhold, F. *NBO Version 4.0*.
- (26) Bader, R. F. W. *Atoms in Molecules: A Quantum Theory*; Clarendon: Oxford, 1990.
- (27) Gilli, G.; Bellucci, F.; Ferretti, F.; Gilli, P. *J. Am. Chem. Soc.* **1989**, *111*, 1023.
- (28) Hobza, P.; Havlas, Z. *Chem. Rev.* **2000**, *100*, 4253.
- (29) Reed, A. E.; Weinhold, F.; Curtiss, L. A.; Pochatko, D. *J. Chem. Phys.* **1986**, *84*, 5687.
- (30) The worse linear fit in ref 7 was due to the mixed vibrational frequencies discussed in ref 7, also pointed out in Figure 6a of this paper.
- (31) (a) Bytheway, I.; Chandler, G. S.; Figgs, B. N. *Acta Crystallogr. A* **2002**, *58*, 451. (b) Galvez, O.; Gomez, P. C.; Pacios, L. F. *J. Chem. Phys.* **2003**, *118*, 4878.
- (32) Koch, U.; Popelier, P. L. A. *J. Phys. Chem.* **1995**, *99*, 9747.
- (33) (a) Alkorta, I.; Elguero, J. *J. Am. Chem. Soc.* **2002**, *124*, 1488. (b) Grabowski, S. J. *J. Phys. Chem. A* **2001**, *105*, 10739.
- (34) Bondi, A. *J. Phys. Chem.* **1964**, *68*, 441.
- (35) Mulliken, R. S. *J. Phys. Chem.* **1952**, *56*, 295.